

Relativistic electronic structure of the NaCl polymorph of CdS[†]

Stanley W. W. Liu and Sohrab Rabii

The Moore School of Electrical Engineering

and The Laboratory for Research on the Structure of Matter, University of Pennsylvania, Philadelphia, Pennsylvania 19174

(Received 11 August 1975)

The energy-band structure of the high-pressure (NaCl) phase of CdS has been calculated using a fully-relativistic symmetrized augmented-plane-wave method. The results have been used to obtain density-of-state histograms over a 30-eV range. Our results indicate that CdS, in this phase, is an indirect-gap semiconductor. The calculated forbidden band gap of 1.5 eV is in good agreement with experimental data. There is, however, no experimental information on the location and nature of the gap for further comparison. The valence band has two nearly degenerate maxima at L and at $(\pi/a)(1,1,0)$ in the Σ directions. The conduction band, similarly, has one minimum at Γ and another set at X with almost the same energy.

I. INTRODUCTION

Cadmium sulfide (CdS) occurs naturally in the hexagonal wurtzite structure and occasionally in the cubic zinc-blende structure under stress; however it undergoes a phase transition to a rock-salt polymorph at high pressures of the order of 30 kbars as shown in Fig. 1. The existence of this phase was originally discovered by Edwards and Drickamer¹ through measurements on the shift of the absorption edge with pressure. Subsequent electrical measurements² and x-ray diffraction studies³ have confirmed the existence of the phase transition and identified the new phase to be of the rock-salt structure. Recently, experimental interest in this phase of CdS has intensified owing to the prospect of retaining this structure in a metastable form even at atmospheric pressures.⁴

In this work, we present the results of an electronic-energy-band structure calculation of the rock-salt phase of CdS, using the symmetrized relativistic augmented-plane-wave (SRAPW) technique. Our motivation for this calculation has been twofold: First, the results obtained should provide us with a model to interpret the increasing number of experimental data being compiled on this phase of CdS; second, the understanding achieved here will hopefully aid us in correlating recent experimental data on the $\text{Pb}_{1-x}\text{Cd}_x\text{S}$ pseudobinary alloy system. It is found experimentally that near the Pb-rich end, this alloy system is in the rock-salt structure, but as the Cd concentration x is increased, it initially develops two phases and eventually crystallizes in the wurtzite structure. With the use of epitaxial thin-film techniques, the rock-salt phase of the alloy has been preserved up to $x=0.38$.⁵

II. METHOD OF CALCULATION

The augmented-plane-wave (APW) technique for solving the one-electron Schrödinger equation in a crystalline solid was first proposed by Slater.⁶

When relativistic effects were recognized to be substantial in certain solids, Conklin *et al.*⁷ introduced a symmetrized perturbation scheme to account for the spin-orbit interaction and other corrections due to the mass-velocity and Darwin terms. The relativistic formulation of the APW technique based on Dirac's equation originated with Loucks⁸ and a symmetrized version, as formulated by Koelling,⁹ serves as the basis for the present calculation.

The use of symmetrization, besides identifying states with the proper symmetry labels, also reduces the size of the basis sets necessary for achieving convergence and thus leading to greater computational economy. Our studies in IV-VI compounds¹⁰ have shown that, provided identical crystal potentials are employed, the above two schemes for relativistic calculations yield results identical within the accuracy of the numerical

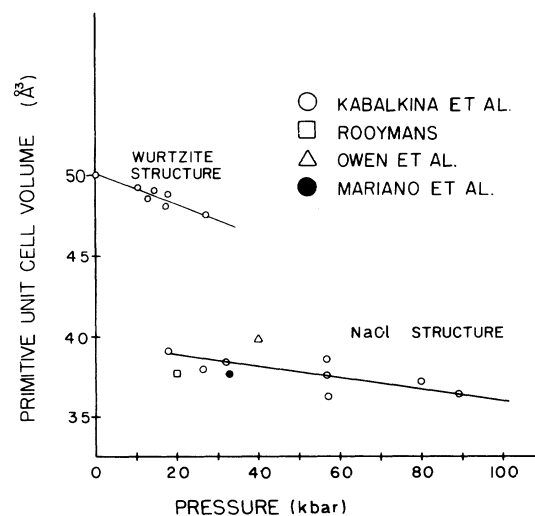


FIG. 1. Variation of the primitive unit cell volume with pressure for CdS.

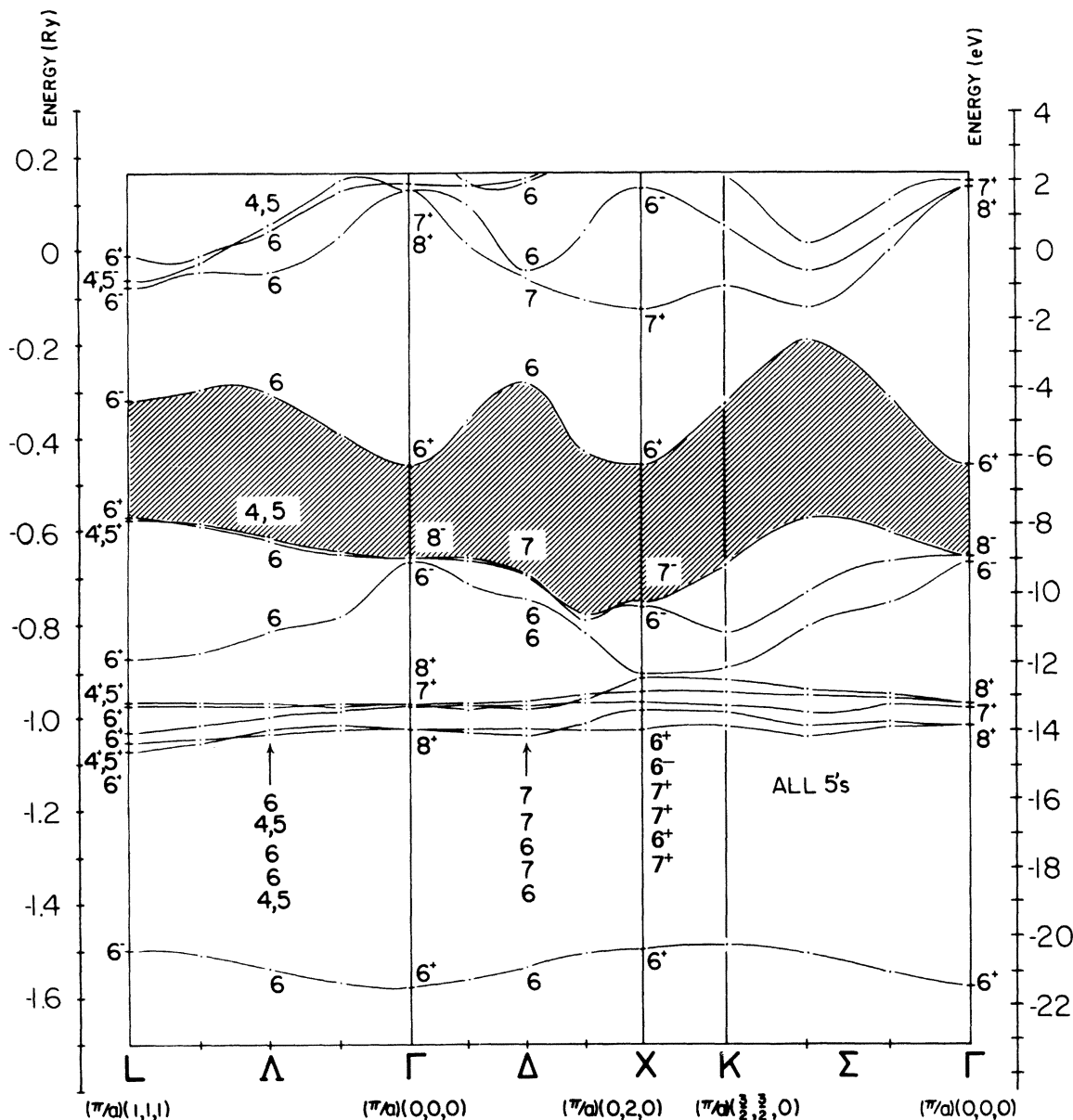


FIG. 2. Energy bands for the NaCl polymorph of CdS in the [010], [111], and [110] directions.

methods, although the latter approach is more convenient in practice. For an extensive review of the RAPW technique, the reader is referred to the article by Dimmock.¹¹

The crystal potential used in our calculation is of the muffin-tin type, which is expected to give reasonable results in view of the close-packed nature of the rock-salt structure. The total Coulomb potential at a given site is given, in the manner of Mattheiss,¹² by a superposition of the potentials due to the atom at that particular site and the contributions from atoms on several neighboring shells. The atomic charge densities used in constructing the muffin-tin potential are

TABLE I. Numerical values for some of the constants used in the calculation.

Lattice constant	10.04345 Bohr radii (5.32 Å)
Radius of APW spheres	2.4765 Bohr radii
Potential in the interstitial region	-0.8967 Ry (-12.2 eV)
Exchange factor within Cd sphere	0.70088
Exchange factor within S sphere	0.72475
Exchange factor for the interstitial region	0.71176

TABLE II. Calculated energy levels for the NaCl polymorph of CdS in units of Ry. The wave vectors are in units of π/a . The energy levels are listed with their symmetry labels for the irreducible representations to their left, except for levels at K and along Σ , where they are all understood to be K_5 and Σ_5 , respectively. Additional labels have been put in only where crossing of levels occurs.

$\Gamma(0,0,0)$	$\Delta(0,\frac{1}{2},0)$	$\Delta(0,1,0)$	$\Delta(0,\frac{3}{2},0)$	$X(0,2,0)$	$\Sigma(\frac{1}{2},0)$	$\Sigma(1,0)$	$K(\frac{3}{2},0)$	$\Lambda(\frac{1}{2},\frac{1}{2})$	$\Lambda(\frac{3}{2},\frac{3}{2})$	$L(0,1,1)$
Γ_7^+ -0.143	Δ_8 0.126	Δ_7 0.150	Δ_6 0.144	X_6^+ 0.132	0.115	0.016	0.164	$\Lambda_{4,5}$ 0.148	Λ_6 -0.018	L_6^- 0.010
Γ_8^+ 0.137	Δ_6 0.105	-0.042	0.074	X_7^+ -0.123	0.037	-0.044	0.054	Λ_6 0.123	$\Lambda_{4,5}$ -0.029	$L_{4,5}^-$ -0.061
	Δ_7 0.032	-0.058	-0.107	X_8^+ -0.455	-0.009	-0.123	-0.077	Λ_6 0.033	-0.045	L_6^- -0.080
Γ_6^+ -0.459	Δ_6 -0.360	-0.280	-0.403	X_6^+ -0.751	-0.308	-0.190	-0.334	Λ_6 -0.386	-0.299	L_6^- -0.314
Γ_8^+ -0.655	Δ_7 -0.663	-0.692	-0.782	X_7^+ -0.759	-0.603	-0.577	-0.676	$\Lambda_{4,5}$ -0.642	-0.613	L_6^- -0.572
	Δ_6 -0.670	-0.699	-0.789	X_8^+ -0.910	-0.669	-0.730	-0.815	Λ_6 -0.647	-0.616	$L_{4,5}^-$ -0.572
Γ_5^+ -0.665	Δ_6 -0.701	-0.742	-0.815	X_6^+ -0.917	-0.757	-0.808	-0.896	Λ_6 -0.782	-0.813	L_6^- -0.873
Γ_8^+ -0.969	Δ_7 -0.967	-0.962	-0.949	X_7^+ -0.942	-0.950	-0.941	-0.920	$\Lambda_{4,5}$ -0.969	-0.965	$L_{4,5}^-$ -0.962
	Δ_6 -0.972	-0.972	Δ_8 -0.966	X_8^+ -0.969	-0.955	-0.951	-0.940	Λ_6 -0.969	-0.966	L_6^- -0.970
Γ_7^+ -0.972	Δ_6 -0.978	-0.982	Δ_7 -0.970	X_6^+ -0.981	-0.974	-0.989	-0.974	Λ_6 -0.973	-0.992	L_6^- -1.031
Γ_8^+ -1.020	Δ_7 -1.019	-1.021	Δ_6 -1.013	X_7^+ -0.981	-1.009	-1.020	-0.985	Λ_6 -1.017	$\Lambda_{4,5}$ -1.047	$L_{4,5}^-$ -1.052
	Δ_6 -1.025	-1.039	Δ_7 -1.022	X_8^+ -1.024	-1.018	-1.040	-1.017	$\Lambda_{4,5}$ -1.023	Λ_6 -1.034	L_6^- -1.071
Γ_6^+ -1.572	Δ_6 -1.560	-1.530	Δ_7 -1.504	X_6^+ -1.496	-1.548	-1.501	-1.487	Λ_6 -1.563	-1.537	L_6^- -1.493

the self-consistent Dirac-Slater relativistic atomic charge densities of Liberman *et al.*¹³ The $X\alpha$ statistical exchange of Slater and Johnson¹⁴ has been used and numerical values for the exchange constants of S and Cd are taken, respectively, from the work of Schwarz¹⁵ and an extrapolation of his results. The lattice constant was chosen to be 5.32 Å, which corresponds to a pressure of 33 kbars, just beyond the phase transition. The parameters used in the calculations are summarized in Table I.

III. RESULTS

A. Energy bands

We have calculated the energy bands over a range of more than 30 eV at twelve points of high symmetry in the Brillouin zone. Figure 2 shows the energy bands in the three high-symmetry directions [100], [111], and [110]. CdS remains a semiconductor even after the pressure-induced phase transition. To test the convergence of the energy levels, we have selected a group of levels near -13.5 eV, which are formed mainly from the 4d electrons of cadmium. Their convergence is expected to be slower than that of other levels. It was found that by using between 50 and 55 SRAPW's, a convergence of better than 0.04 eV has been achieved even in the Σ direction, which has the lowest symmetry in this group (Fig. 3). For levels of higher symmetry, fewer basis functions were necessary to achieve the same or better convergence. The energy levels in the -21.5-3.6-eV interval calculated at these twelve high-symmetry points are given in Table II. The symmetry notation for points in the Brillouin zone of the face-centered cubic lattice are those of Bouckaert *et al.*,¹⁶ while the notation for the

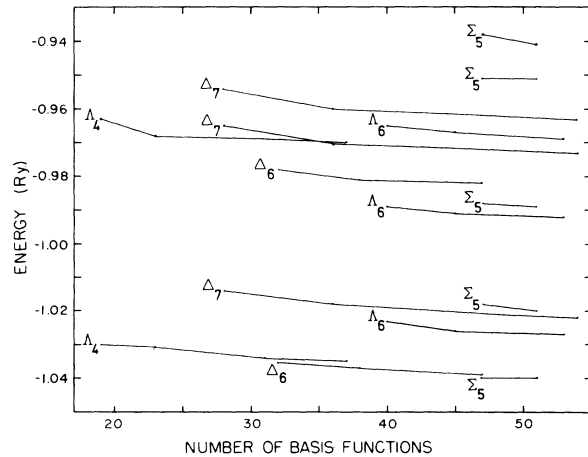


FIG. 3. Convergence of the cadmium 4d levels as a function of the number of SRAPW's used in the expansion of the wavefunctions.

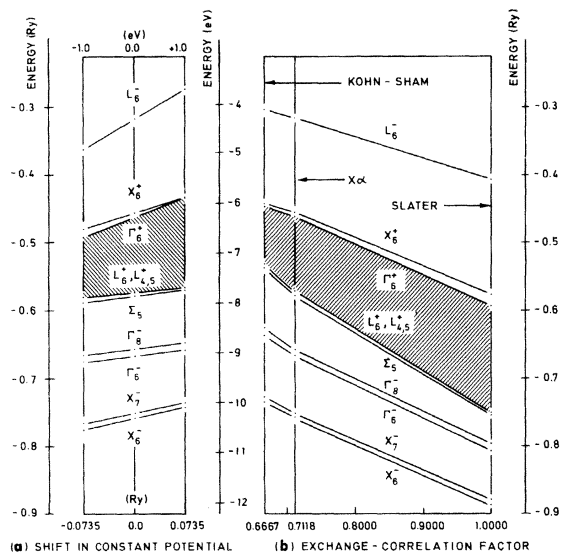


FIG. 4. Variation of the energy levels in the vicinity of the gap, (a) with changes in the interstitial potential relative to the calculated value, (b) as a function of the exchange-correlation factor.

double-group representations are due to Elliot.¹⁷

The constant potential in the interstitial region between the APW spheres is a calculated quantity that results from the volume averaging of the actual crystal potential in the interstitial region. Sometimes this quantity is used as an adjustable parameter to match one of the calculated results, such as the minimum gap, to the experimental data. Although we have found no need to do so in our calculation, we have varied the constant potential by a relatively large value of 1 eV (0.0735 Ry) on each side of the calculated value in order to determine its effect on a few selected energy levels about the forbidden gap. The results are shown in Fig. 4(a). One observes that the shift in energy levels is linearly proportional to the shift in the constant potential. In the range under consideration, there is no change in the symmetry labels of the fundamental band gap, which remains indirect. For a typical adjustment of the constant potential (i. e., a few tenths of an electron volt), the corresponding change in the calculated forbidden gap is less than 5%.

In order to study the effect of the particular choice of the exchange-correlation factor on our results, the same set of energy levels, used in the constant potential shift studies, were also calculated using two other prescriptions for the exchange, ranging from the Slater¹⁸ exchange factor of $\alpha = 1$ to the Kohn-Sham¹⁹ exchange factor of $\alpha = \frac{2}{3}$. The results are shown in Fig. 4(b). Except near the band edges, the shift in energy levels is roughly proportional to the value of the

exchange factor. As expected, the results using the Kohn-Sham exchange are closer to our $X\alpha$ results than those with the Slater exchange. The band gap with the Kohn-Sham exchange is 11% lower than our $X\alpha$ results.

B. Density of states

We have also extended our energy-band calculations to ten more points of lower symmetry in the Brillouin zone. The projection operators needed in symmetry determination were readily obtained for these additional points by using the method of ray representations of Hurley.²⁰ The group of the \vec{k} vector for seven of these ten points consists of only two operations and the corresponding one-dimensional irreducible representations are degenerate by time-reversal symmetry. Although we do not expect their convergence to be quite as good, our studies on the compatibility relations and the connecting of the levels along all symmetry lines in the Brillouin zone indicate that it is satisfactory. Altogether, we have taken 20 points in $\frac{1}{48}$ of the Brillouin zone giving the equivalent of 256 regularly spaced points in the full Brillouin zone; with these results, we have constructed an energy density of states by a commonly used histogram method.²¹

Table III lists all 20 symmetry points considered. In the calculations of the histograms, we have introduced a three-point smoothing to reduce scattering of the data and to make the density of states less sensitive to location of the bins relative to the energy bands. In the choice of the proper energy bin size, we have to optimize between resolution of the bands and the stability against small shifts in the relative location of the bins. With an energy bin size of 0.04 Ry, we find that the shape of the histograms is still not too stable with respect to shifts in the location of the mesh points relative to the energy eigenvalues. After testing a series of other bin sizes, we believe that the final choice of 0.01 Ry gives a realistic representation of the density of states, as shown in Fig. 5. This bin size is sufficiently large so that the statistical fluctuations appear still to be within reasonable limits.

IV. DISCUSSION

We find that CdS in the rock-salt structure with a lattice constant of 5.32 Å is indeed a semiconductor with an indirect band gap of 1.5 eV. The valence band has two nearly degenerate sets of maxima, at L and in the $[110]$ direction, while the conduction band has nearly degenerate minima at Γ and at X . Near the bottom of the first conduction band, a X_6^+ level is nearly degenerate with a Γ_6^+ level, while near the top of the valence band, a Σ_5 level is nearly degenerate with a L_6^+ level and

TABLE III. Listing of the 20 points in $\frac{1}{48}$ of the first Brillouin zone used to construct the density-of-states histogram. The wave vectors are listed in units of π/a .

Wave vector	Order of the group of \vec{K}	Multiplicity	Wave vector	Order of the group of \vec{K}	Multiplicity
$\Gamma(0, 0, 0)$	48	1	$\Sigma(1, 1, 0)$	4	12
$X(0, 2, 0)$	16	3	$U(\frac{1}{2}, 2, \frac{1}{2})$	4	8
$L(1, 1, 1)$	12	4	$Z(\frac{1}{2}, 2, 0)$	4	12
$\Delta(0, \frac{1}{2}, 0)$	8	6	$C(1, 1, \frac{1}{2})$	2	24
$\Delta(0, 1, 0)$	8	6	$J(\frac{1}{2}, 1, \frac{1}{2})$	2	24
$\Delta(0, \frac{3}{2}, 0)$	8	6	$J(\frac{1}{2}, \frac{3}{2}, \frac{1}{2})$	2	24
$W(1, 2, 0)$	8	6	$O(\frac{1}{2}, 1, 0)$	2	24
$\Lambda(\frac{1}{2}, \frac{1}{2}, \frac{1}{2})$	6	8	$O(\frac{1}{2}, \frac{3}{2}, 0)$	2	24
$K(\frac{3}{2}, \frac{3}{2}, 0)$	4	4	$O(1, \frac{3}{2}, 0)$	2	24
$\Sigma(\frac{1}{2}, \frac{1}{2}, 0)$	4	12	$Q(1, \frac{3}{2}, \frac{1}{2})$	2	24

the $L_{4,5}^+$ level near by. The calculated minimum band gap of 1.5 eV is half-way between the experimentally measured thermal gap of ~ 1.3 eV of Samara and Giardini² and the optical gap of ~ 1.7 eV of Edwards and Drickamer.¹ About 5.3 eV above the top of the valence band, there is a secondary gap of 0.8 eV in width.

Wave functions calculated in our earlier nonrelativistic symmetrized APW calculations²² on CdS have been used to identify the principal compo-

nents of selected energy-band states. In the density-of-state histogram, the cadmium d levels show up clearly as a band with a width of 1.6 eV centered at -13.5 eV. The peaks due, respectively, to the Γ_8^+ (Γ_{12}) and Γ_7^+ (Γ_{25}') levels and to the Γ_8^+ (Γ_{25}') level have been resolved. Over 90% of this band comes from the cadmium $4d$ levels. The lower isolated band centered at -20.5 eV, near the Γ_6^+ (Γ_1) level, is s -like with 75% of the contribution coming from the sulfur $3s$ levels. The peak centered at -11.2

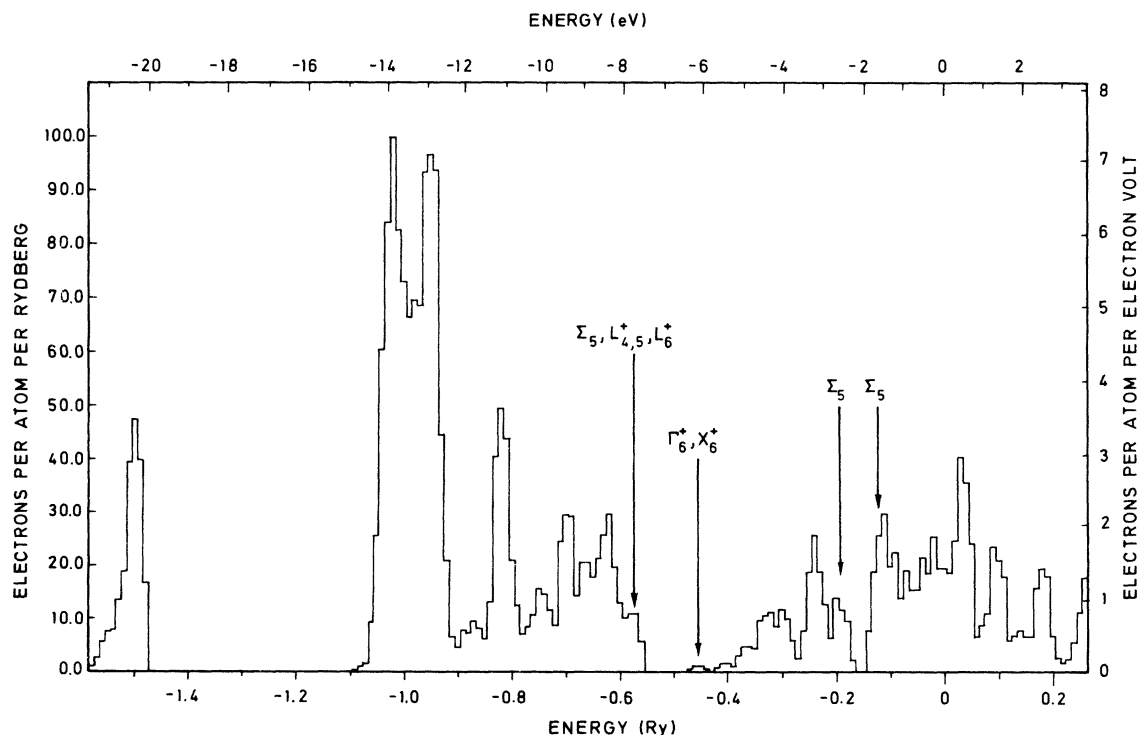


FIG. 5. Density-of-States histogram for the NaCl polymorph of CdS.

eV is due mainly to a clustering of energy eigenvalues along the line joining point Δ at (π/a) $(0, \frac{3}{2}, 0)$ and point K at $(\pi/a)(\frac{3}{2}, \frac{3}{2}, 0)$ in the first Brillouin zone. Examination of the wave functions of the $\Delta_6(\Delta_1)$ and the K_5 levels indicates that this peak consists of roughly equal contributions from the cadmium $4d$ levels and the sulfur $3p$ levels. Near the top of the valence band, almost 70% of the density of states comes from the sulfur $3p$ levels with 20% cadmium $4d$ levels mixed in. The bottom of the first conduction band is found to be mainly s -like in the Cd and S spheres with about half of the charge in the interstitial region. We observe that the gaps in the density of states are slightly smaller than those shown in the energy

band diagram. This is due to the fact that the energy levels in the low-symmetry directions "spill" into the gap resulting in narrower effective energy gaps. However, this narrowing effect may be partly due to poorer convergence of the energy levels in the low-symmetry directions and partly due to the smoothing process in the calculation of the histograms.

ACKNOWLEDGMENTS

We are grateful to Dr. Dale D. Koelling for generously providing us with his version of the Symmetrized Relativistic APW programs. Thanks are due to Dr. Robert H. Lasseter and Dr. Cary Y. Yang for many helpful discussions.

[†]Supported by the Laboratory for Research on the Structure of Matter and ARPA of DOD as monitored by the Air Force Office of Scientific Research under Contract No. F44620-75-C-0069 and by NSF under Grant No. DMR72-03025.

¹A. L. Edwards and H. G. Drickamer, *Phys. Rev.* **122**, 1149 (1961).

²G. A. Samara and H. G. Drickamer, *J. Phys. Chem. Solids* **23**, 457 (1962); G. A. Samara and A. A. Giardini, *Phys. Rev.* **140**, A388 (1965).

³C. J. M. Rooymans, *Phys. Lett.* **4**, 186 (1963); N. B. Owen, P. L. Smith, J. E. Martin, and A. J. Wright, *J. Phys. Chem. Solids* **24**, 1519 (1963); P. L. Smith and J. E. Martin, *Phys. Lett.* **6**, 42 (1963); A. N. Mariano and E. P. Warekois, *Science* **142**, 672 (1963); S. S. Kabalkina and Z. V. Troitskaya, *Dokl. Akad. Nauk SSSR* **151**, 1068 (1963) [*Sov. Phys. - Doklady* **8**, 800 (1964)]; W. C. Yu and P. J. Gielisse, *Mat. Res. Bull.* **6**, 621 (1971).

⁴Z. V. Malyushitskaya, S. S. Kabalkina, and L. F. Vereschchagin *Fiz. Tverd. Tela* **14**, 1219 (1972) [*Sov. Phys. - Solid State* **14**, 1040 (1972)]; F. J. Bogacki and T. E. Thompson, *Bull. Am. Phys. Soc.* **20**, 449 (1975).

⁵K. Wu, Ph. D. thesis (University of Pennsylvania, 1971) (unpublished); A. K. Sood, Ph. D. thesis (University of Pennsylvania, 1975) (unpublished).

⁶J. C. Slater, *Phys. Rev.* **51**, 846 (1937).

⁷J. B. Conklin, Jr., L. E. Johnson, and G. W. Pratt, Jr., *Phys. Rev.* **137**, A1282 (1965).

⁸T. L. Loucks, *Phys. Rev.* **139**, A1333 (1965).

⁹D. D. Koelling, *Phys. Rev.* **188**, 1049 (1969).

¹⁰R. H. Lasseter and S. Rabii (unpublished).

¹¹J. O. Dimmock, *Solid State Physics*, edited by H. Ehrenreich, F. Seitz, and D. Turnbull (Academic, New York, 1971), Vol. 26, p. 103.

¹²L. F. Mattheiss, *Phys. Rev.* **133**, A1399 (1964).

¹³D. Liberman, J. T. Waber, and D. T. Cromer, *Phys. Rev.* **137**, A27 (1965).

¹⁴J. C. Slater and K. H. Johnson, *Phys. Rev. B* **5**, 844 (1972).

¹⁵K. Schwarz, *Phys. Rev. B* **5**, 2466 (1972).

¹⁶L. P. Bouckaert, R. Smoluchowski, and E. P. Wigner, *Phys. Rev.* **50**, 58 (1936).

¹⁷R. J. Elliott, *Phys. Rev.* **96**, 280 (1954).

¹⁸J. C. Slater, *Phys. Rev.* **81**, 385 (1951).

¹⁹W. Kohn and L. J. Sham, *Phys. Rev.* **140**, A1133 (1965); R. Gaspar, *Acta Phys. Acad. Soc. Hung.* **3**, 263 (1954).

²⁰A. C. Hurley, *Proc. R. Soc. Lond.* **260**, 1 (1966).

²¹D. Brust, *Phys. Rev.* **134**, A1337 (1964); R. H. Lasseter, Ph. D. thesis (University of Pennsylvania, 1972).

²²S. W. W. Liu and S. Rabii (unpublished).